Purinergic regulation of guinea pig suburothelial myofibroblasts

C. Wu[1], G. P. Sui[2] and C. H. Fry[2]

[2] *Institute of Urology & Nephrology and* [1] *Department of Medicine, University College London, 48 Riding House Street, London W1W 7EY, UK*

The Ca^{2+}-regulating and electrophysiological properties of guinea-pig suburothelial myofibroblasts have been measured in order to investigate their potential role in the sensation of bladder fullness, due to their strategic position between the urothelium and afferent fibres. Previous work has shown that stretch of the bladder wall releases ATP. Cells that stain positively for vimentin were isolated. About 45% of cells (median membrane capacitance 13.3 pF) exhibited spontaneous depolarizations to about −25 mV with a physiological Cl^- gradient (frequency $2.6 \pm 1.5\ min^{-1}$, duration 14.5 ± 2.2 s, $n = 15$). Under voltage-clamp spontaneous inward currents (frequency $1.5 \pm 0.2\ min^{-1}$, duration 14.5 ± 7.0 s, $n = 18$) were recorded, with a similar reversal potential. The spontaneous currents were preceded by intracellular Ca^{2+} transients with a magnitude that was independent of membrane potential. All cells tested responded to ATP by generating an intracellular Ca^{2+} transient, followed by inward currents; the currents had a similar reversal potential and slope conductance to their spontaneous counterparts. ATP-generated transients were mimicked by UTP and ADP but not by α,β-methylene-ATP (1–10 μM) or CTP (30 μM), indicating that ATP acts via a P2Y receptor. Transients were partially attenuated by 1 mM suramin but PPADS (80 μM) had no effect. These data indicate that ATP acts via a P2Y receptor, but responses were resistant to the $P2Y_1$ antagonist MRS2179. ATP-generated transients were abolished by intracellular perfusion with heparin and TMB-8 indicating that IP_3 was the intracellular second messenger. The reversal potentials of the spontaneous and ATP-generated currents were shifted by about +45 mV by a 12-fold reduction of the extracellular $[Cl^-]$ and the currents were greatly attenuated by 1 mM DIDS. No transients were generated on exposure to the muscarinic agonist carbachol. We propose that these cells may play a regulatory step in the sensation of bladder fullness by responding to ATP. The precise mechanism whereby they couple urothelial ATP release to afferent excitation is the next step to be elucidated.

(Resubmitted 10 May 2004; accepted after revision 25 June 2004; first published online 2 July 2004)

Corresponding author C. H. Fry: The Institute of Urology and Nephrology, 48 Riding House Street, London W1W 7EY, UK. Email: c.fry@ucl.ac.uk

Perception of bladder fullness is a vital step in initiating the micturition reflex. Basically myelinated afferents from the bladder wall ultimately convey information about bladder volume to the brainstem, which then modulates sacral output to the bladder and internal sphincter (De Groat & Yoshimura, 2001; Fowler, 2002). In a large number of people inappropriate sensations of bladder fullness can lead to symptoms of urinary urge, increased frequency of micturition, and even urinary incontinence (Donovan *et al.* 1999). There is therefore a clinical imperative to understand the physiological basis of the micturition reflex.

The precise cellular and tissue mechanism whereby increased bladder filling is translated into afferent activation is poorly understood. A crucial observation is that changes to hydrostatic pressure across the bladder wall lead to baso-lateral release of ATP, and that this process is mediated by urothelial Na^+ transport through amiloride-sensitive channels (Ferguson *et al.* 1997). The ATP was surmised to activate suburothelial afferents. This hypothesis was strengthened by the localization of $P2X_3$ receptors on suburothelial nerves (Lee *et al.* 2000) and the fact that $P2X_3$ knock-out mice exhibit urinary retention – presumably due to attenuation of the sensory mechanism (Cockayne *et al.* 2000). Furthermore a link to pathological conditions has been proposed from the observation that more ATP is released from urothelium of patients with heightened symptoms of urinary urge (Kumar *et al.* 2004).

 DOI: 10.1113/jphysiol.2004.067934

Recently we, and others, have identified a distinct suburothelial layer of cells that have the microscopical and immunocytochemical characteristics of myofibroblasts (Sui *et al.* 2002; Wiseman *et al.* 2003). Typically these cells stain for the intermediate filament protein vimentin and moreover are the main locus for the gap junction protein connexin43 (Cx43). In addition, these cells make very close appositions to suburothelial afferents and earlier work has suggested that a similar layer of cells may be the terminus of efferent nitrergic nerves (Smet *et al.* 1996). Isolated cells generate spontaneous depolarizing spikes and furthermore application of ATP elicits not just inward currents, but also transient increases of the intracellular $[Ca^{2+}]$ (Sui *et al.* 2004). Overall these cells are ideally placed to play a modulatory role in the process of bladder sensation: they form a dense electrical network in a space between the urothelium and afferent nerves; they respond to the putative sensory transmitter ATP; they may be the target for modulatory nitrergic nerves; and their physical apposition to afferent fibres provides a mechanism to activate these fibres. We have suggested that these cells are an intermediate and variable gain stage in the process of bladder fullness sensation. However, there has been no detailed characterization of the electrical properties of these cells, or their response to purinergic agonists and this was the aim of the present study.

Methods

Cell preparation

Guinea-pig bladders were used after the animals were killed by procedures in accordance with the UK Animals (Scientific Procedures) Act 1986. The urothelium was separated from the underlying detrusor layer by blunt dissection under × 10–20 magnification. Samples were digested at 37°C with a nominally Ca^{2+}-free collagenase-based medium, previously described for the preparation of isolated human detrusor myocytes (Montgomery & Fry, 1992) and with constant stirring for 30 min. After treatment the tissue was partially disrupted and two main cell types could be seen under a light microscope, (a) large round urothelial cells and (b) a layer of ovoid or spindle-shaped cells, with or without one or more dendrite-like structures. The latter cells were used for experimental recording. Some of the latter cells were stained for the intermediate filament vimentin.

Solutions

Bladder wall samples were used immediately for experiments and placed in a nominally Ca^{2+}-free, Hepes-buffered solution of the following composition (mM): NaCl, 105.4; $NaHCO_3$, 22.3; KCl, 3.6; $MgCl_2$, 0.9; NaH_2PO_4, 0.4; Hepes, 19.5; glucose 5.4; sodium pyruvate, 4.5; pH 7.1. Cells were superfused at 37°C with Tyrode solution (mM): NaCl, 118; KCl, 4.0; $NaHCO_3$, 24; NaH_2PO_4, 0.4; $MgCl_2$, 1.0; $CaCl_2$, 1.8; glucose, 6.1; sodium pyruvate, 5.0; gassed with 5% CO_2–95% O_2, pH 7.4. For the low-Cl^- solution ($[Cl^-]$ reduced from 127.6 mM to 10.7 mM), the NaCl of the Tyrode solution was replaced by equimolar sodium isethionate; the $CaCl_2$ was increased from 1.8 to 2.34 mM to maintain a constant Ca^{2+} activity (Fry & Langley, 2001). Na_2ATP, $Na_{1.5}ADP$, Na_3UTP, α,β-methylene-ATP (ABMA), MRS2179, niflumic acid, cytidine triphosphate-Na_2 (CTP), suramn-Na_6, pyridoxal phosphate-6-azo(benzene-2,4-disulphonic acid)-Na_4 (PPADS) and 4-acetamido-4′-isothiocyanato-2,2′-stilbenedisulphonic acid (SITS) were added to the superfusate from aqueous stocks. 4,4′-Diisothiocyanatostilbene-2,2′-disulphonate (DIDS) was diluted to a final concentration of 1.2 mM to give a working concentration of 1 mM, due to an 80% purity. All chemicals were from Sigma UK. 8-(*N*,*N*-Diethylamino)-octyl-3,4,5-trimethoxybenzoate (TMB-8; Calbiochem) was added to Tyrode solution to achieve a final concentration of 100–200 μM.

Immunohistochemical staining

Samples of cells that would otherwise have been used for experimental recording were stained for vimentin using mouse mAb 3B41112 457 (Boehringer Mannheim, UK, 1 : 100) and AP 192C donkey anti-mouse IgG as a secondary antibody conjugated to Cy3 (Chemicon Int Ltd, UK, 1 : 250). Cells were illuminated with an argon laser at 543 nm and emission recorded at 570 nm using a Bio-Rad Radiance 2100 system, further details are as previously described (Sui *et al.* 2002).

Electrophysiological recordings

These were made using patch-type pipettes (3–4 MΩ) made from borosiliate glass and filled with a Cs-filling solution of the following composition (mM): CsCl 20; aspartic acid, 110; $MgCl_2$, 5.45; Na_2ATP, 5.0; Na_4GTP, 0.1; EGTA, 0.1; Hepes, 5.0, pH adjusted to 7.1 with CsOH. For some experiments a K-filling solution was used in which KCl replaced CsCl and KOH was used to adjust pH to 7.1. In some experiments low-molecular mass heparin (Sigma) was added to Cs^+-based pipette filling solutions to a final concentration of 4 mg ml^{-1}. Membrane potentials were recorded in current-clamp mode, resting potentials were recorded with no current passed into the cells ($I_h = 0$), ionic currents were recorded under voltage-clamp. An Axopatch-1D system (Axon Instruments) was used for experiments and data recorded via an A/D converter (Digidata 1200, Axon Instruments) at 4 kHz, and filtered with a low-pass filter of cut-off frequency 2 kHz. To investigate the effect of ATP on

net ionic current a holding potential (V_h) of −60 mV was used as this was close to the average resting membrane potential (see Results). Cell capacitance (c_m) was measured from the integral of the voltage response to a small current injection. Cell input resistance (r_{inp}) was calculated from the steady-state voltage response (V) to a current injection (i; $r_{inp}, = V/i$) and the membrane time constant (τ_m) from the rising profile. Specific membrane resistance (R_m; Ω cm^2) was calculated from the relationship $\tau_m = R_m C_m$, where C_m is the specific membrane capacitance (1 μF cm^{-2}; Weidmann, 1970). Cell surface area (a) was calculated from the cell capacitance (c_m) by the relationship $a = c_m/C_m$. Outwardly rectifying current–voltage relationships over an extended voltage range (Fig. 9*B*) were fitted to a model of a channel with a single barrier according to Eyring's rate theory (Eyring, 1936)

$$I = k_1(\exp(-k_2))\{([Cl^-]_o \exp(\gamma V k_3)) - ([Cl^-]_i \exp(-\gamma V k_3))\} \quad (1)$$

where k_1, k_2 and k_3 are constants, and $[Cl^-]_o$ and $[Cl^-]_i$ are the superfusate and pipette $[Cl^-]$, respectively. γ is a constant.

Measurement of the intracellular [Ca^{2+}]

In some experiments the intracellular $[Ca^{2+}]$ ($[Ca^{2+}]_i$) was recorded simultaneously with electrophysiological data. In this case 100 μM K_5Fura-2 was added to the pipette filling solution, and the [EGTA] was 50 μM. We have shown previously (Wu & Fry, 2001) in detrusor smooth muscle cells that these concentrations of Ca^{2+} buffers contribute about 10% to the total Ca^{2+}-buffering power of the cell. Furthermore qualitatively similar observations were made in some cells in which 50 μM K_5Fura-2 was used. Cells were excited at 340/380 nm at 50 Hz and the fluorescence intensity recorded between 410 and 480 nm. The Fura-2 signal was calibrated using solutions of varying $[Ca^{2+}]$ in the absence of cells as previously described (Wu *et al.* 2002).

Data presentation and calculations

Data groups are quoted as mean values ± S.D. or S.E.M., except when data sets were not normally distributed, when median values (± 25% interquartiles) are given. Significances between data sets were tested using Student's t test; the null hypothesis was rejected at $P < 0.05$. Skewness (g_1, third moment of the mean) values of data sets were calculated using KaleidaGraph (Synergy Software). t_s values for a normal distribution were calculated from g_1/N where:

$$N = \sqrt{\{6n(n-1)\}/\{(n-2)(n+1)(n+3)\}} \quad (2)$$

and n = number of observations.

Results

Cellular characteristics

The cells were spindle-shaped, ovoid or round in appearance, and a subset of these that would have been used for experiments were stained for vimentin: all such cells showed positive staining. The resting potential was recorded just after membrane breakthrough in a sample of cells using K^+-filled electrodes, to yield a value of −61 ± 14 mV ($n = 20$). A similar value was measured using Cs^+-filled electrodes just after membrane breakthrough, but after several seconds the recorded potential approached about −30 mV, and remained stable at this value if no current was injected into the cell. Figure 1 shows histograms of the values of different electrical characteristics recorded from 68 cells: membrane capacitance, c_m (Fig. 1*A*, $n = 68$); membrane time constant, τ_m (Fig. 1*B*, $n = 61$); and input resistance, r_{inp} (Fig. 1*C*, $n = 61$). The skewness coefficients (g_1) were positive and shown by the histograms; the calculated t_s values (g_1/N; see Methods) were, respectively, 5.57, 4.72 and 8.19, and significantly ($P < 0.001$) different from zero showing that the histograms are skewed to the right. The median (25%, 75% interquartile) values were, respectively: c_m = 13.3 pF (9.0, 19.1 pF), τ_m = 70 ms (46, 104 ms); r_{inp} = 5.3 GΩ (3.0, 9.7 GΩ). The median surface area of the cell ($= c_m/C_m$) was 1350 μm^2 and the median specific membrane resistance ($= \tau_m/C_m$) was 7.0×10^4 Ω cm^2. The following results, however, showed no dependence on the absolute values of the above electrical characteristics. Thus, there was no evidence that the cells in the right-hand tail of the distribution represented a different functional subset of the cell population.

Spontaneous membrane potential and current events

Figure 2*A* shows typical tracings of membrane potential and current recorded from a suburothelial myofibroblast with a Cs^+-filled pipette. In the first half of the trace, recordings were made under current-clamp conditions with a small holding current. Spike-like depolarizations, which did not overshoot but tended to approach −30 mV in this example, were superimposed on a more negative resting level of about −60 mV. A switch to voltage-clamp in the second part of the trace to a holding potential of −60 mV showed spontaneous inward currents of similar frequency. Spontaneous currents under voltage-clamp were recorded in 44.8% of cells investigated.

Figure 2*B* shows a tracing in which spontaneous inward currents were recorded during variation of the holding potential from −60 mV to +20 mV. As the holding potential became less negative the magnitude of the currents became smaller and finally reversed to become an outward current. Figure 2*C* shows the mean

current–voltage relationship from seven cells. The data over this relatively limited voltage range were fit to a straight line, which yielded a reversal potential, E_{rev}, of -25.4 ± 8.5 mV, and a mean slope conductance, g, of 0.76 ± 0.21 nS pF^{-1}.

The characteristics (mean ± s.e.m.) of the spontaneous membrane potential ($\Delta E_m > 20$ mV) and current (> 100 pA) events were measured. In 15 cells 89 spontaneous depolarizations were analysed which occurred with a mean frequency of 2.6 ± 0.7 min^{-1}. The mean starting potential was -62.4 ± 2.7 mV with a peak value of -24 ± 2.0 mV (amplitude 38.4 ± 2.8 mV). The mean duration (to 90% repolarization) was 14.5 ± 2.2 s, with a repolarization time constant of 3.8 ± 0.7 s. Spontaneous currents ($n = 102$, 18 cells) from a holding potential of −60 mV occurred at a mean frequency of 1.5 ± 0.2 min^{-1} of amplitude 386 ± 91 pA. Their duration (to 90% decay) was 14.5 ± 7.0 s, with a time constant of 4.2 ± 1.0 s. The frequency, duration and time constant of the membrane potential and current fluctuations were not significantly different. The final amplitude of the membrane depolarizations was also not significantly different from the reversal potential of the current transients. These observations are consistent with the hypothesis that the spontaneous currents underlie the fluctuations of membrane potential.

Intracellular Ca^{2+}, $[Ca^{2+}]_i$, and spontaneous inward currents

To gain more insight into the characteristics of the spontaneous inward currents, $[Ca^{2+}]_i$ was measured simultaneously. Figure 3*A* shows a close association between the generation of inward currents and Ca^{2+} transients. Furthermore removal of extracellular Ca^{2+} (omission of $CaCl_2$ and addition of 0.1 mM EGTA) reversibly suppressed both phenomena.

One question is to determine the causal relationship between the inward current and Ca^{2+} transient. Figure 3*B* shows that variation of the holding potential altered the magnitude and polarity of the current, but had no significant effect on the magnitude of the Ca^{2+} transient. This suggests that the Ca^{2+} transient was not generated by the current, but rather the Ca^{2+} transient occurred spontaneously and in consequence generated a current.

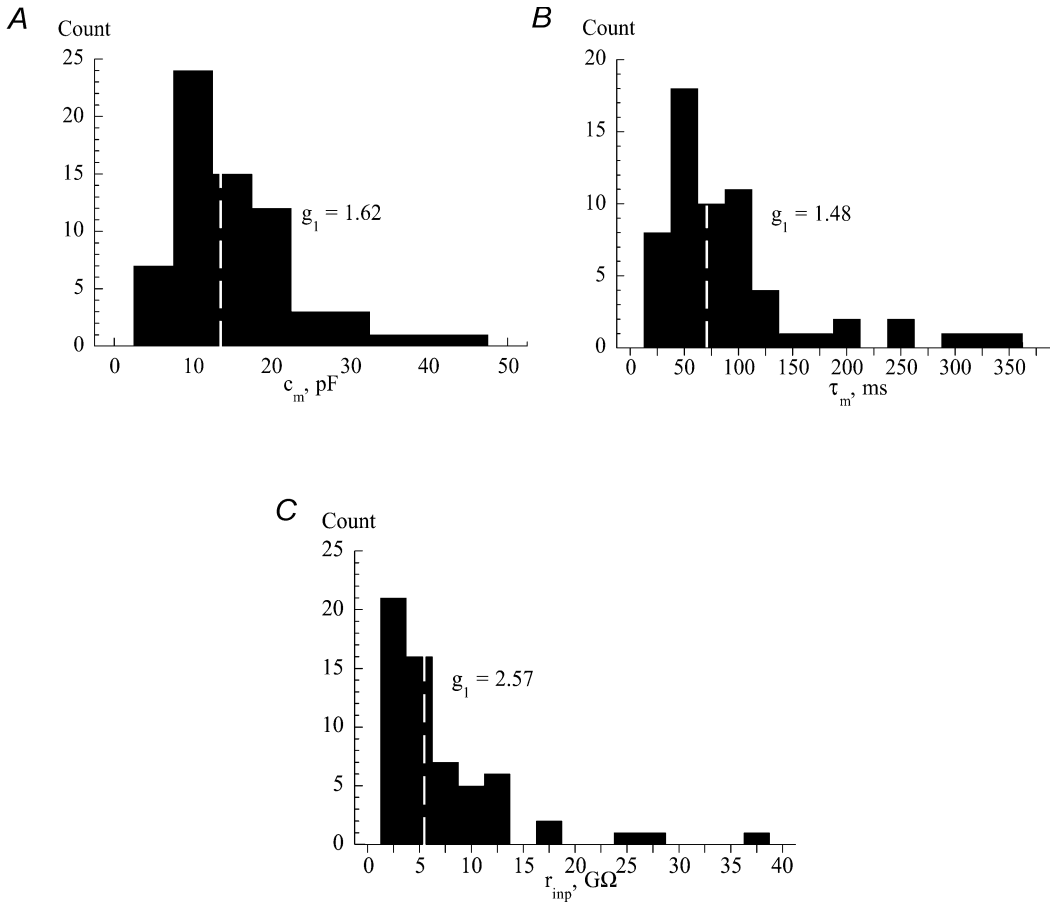

Figure 1. Histograms of electrical characteristics of guinea-pig suburothelial myofibroblasts
A, membrane capacitance, c_m. *B*, membrane time constant, τ_m. *C*, input resistance, r_{inp}. The white dotted line in each part shows the median value. The skewness values, g_1, of each data set are shown in the relevant part.

This was corroborated by the phase-plane plot shown in Fig. 3*C*, which shows the relationship between $[Ca^{2+}]_i$ and current during a single pair of transients. The arrows show the time course of the phenomena and demonstrates that the rise of $[Ca^{2+}]_i$ preceded the initiation of the current transient. The inset shows the data from which the phase-plane plot was derived, with the figures equivalent to the numbered points on the loop.

The association between Ca^{2+} transients and transient currents was evident also in the magnitude of the respective events. Figure 4 plots data from a representative cell and shows a positive relationship between the magnitudes of the two events, thus the inward current does not represent an all-or-none event but a graded response.

ATP-generated responses

Exogenous ATP has been shown previously to elicit, in separate observations, Ca^{2+} transients and inward currents (Sui *et al.* 2004). The experiments below were designed to show if these phenomena showed similarities to the above spontaneous transient responses. Figure 5*A* shows a record of simultaneous measurement of $[Ca^{2+}]_i$ and ionic current in a cell clamped at −60 mV on application of ATP between 0.1 μM and 100 μM. The lowest concentration was effective in eliciting small responses with a maximal response attained at 10 μM. A higher [ATP] (100 μM) did not appear to cause desensitization of either response, as judged by the peak magnitudes, although the time course was somewhat attenuated. As with the spontaneous responses there was a positive relationship between the magnitudes of inward current and Ca^{2+} transient.

Several other similarities were noted between the ATP-generated and spontaneous events. Figure 5*B* shows that the magnitude and polarity of the current were functions of membrane potential, whereas the Ca^{2+} transient was independent of E_m. The reversal potential of the current in this cell was at −24 mV and in nine cells the mean value was -28.7 ± 7.9 mV, with an average slope conductance, calculated from a linear fit of the data, of 0.73 ± 0.18 nS pF^{-1}. These values were not significantly different from the mean reversal potential and slope conductance of the spontaneous currents.

Figure 5*C* shows that a similar temporal relationship existed between the ATP generated and spontaneous events. A phase-plane plot of a pair of transients elicited by 100 μM ATP shows that membrane current was generated only after the rise of $[Ca^{2+}]_i$ had been initiated.

If the transient currents evoked by ATP are sufficiently large to influence the membrane potential, the addition of ATP should depolarize or hyperpolarize the cell, depending on the initial resting value. Figure 5*D* shows responses from six different cells in which the membrane potential was altered under current clamp with 100 μM ATP added. When cells were current-clamped to more negative potentials (i.e negative to about −30 mV) they depolarized, and conversely they hyperpolarized when clamped to potentials positive to about −20 mV. The null potential, as estimated from the individual experiments in Fig. 5*D*, was -23.1 ± 3.8 mV and is very similar to the reversal potential of the ATP-induced current. This result indeed suggests that the ATP-induced current plays a predominant role in determining the overall membrane potential of the cell.

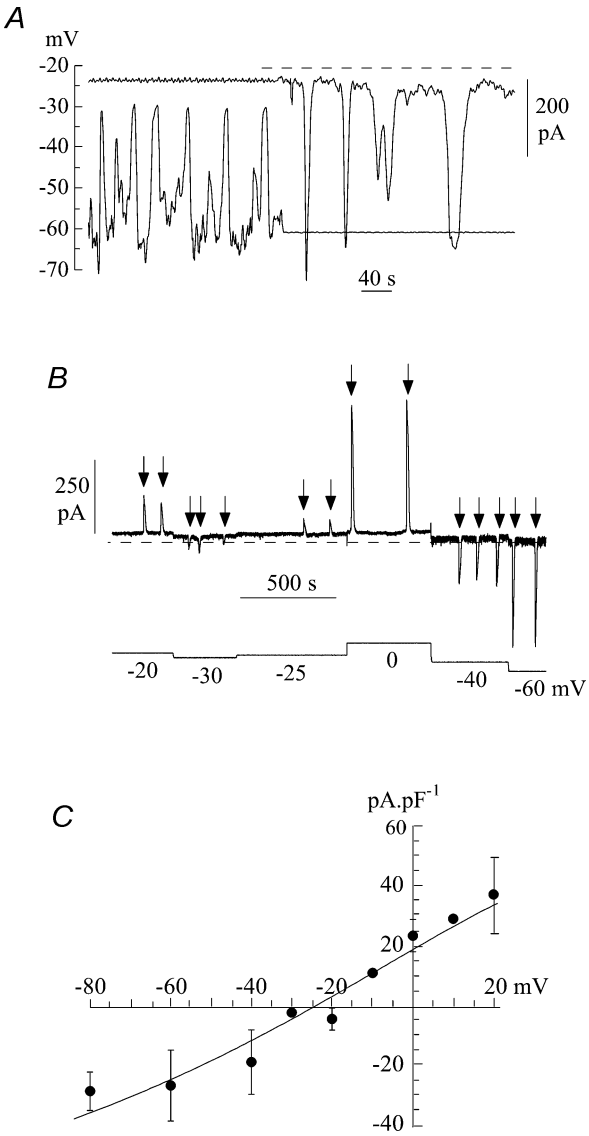

Figure 2. Spontaneous currents in suburothelial myofibroblasts
A, current- and voltage-clamp recordings from an isolated cell using a Cs^+-filled pipette. The first half of the record is under current-clamp; the second half shows ionic current recorded when voltage-clamped at −60 mV. Dotted line shows the zero-current level. *B*, voltage dependence of spontaneous currents under voltage-clamp: holding potential was varied between −60 and 0 mV in this example in a series of steps. Spontaneous currents are arrowed. *C*, current–voltage relationship of spontaneous currents from seven cells. Mean ± S.D. of data; the straight line was fitted by least-squares analysis of the mean data.

The dependence of membrane currents on the $[Ca^{2+}]_i$ and sources of intracellular Ca^{2+}

The previous experiments indicate that ATP-induced Ca^{2+} transients are generated by release from intracellular sources. The signalling pathway was further explored by examining the effects of intracellular heparin or superfusion with TMB-8. These agents interfere with IP_3-dependent pathways for intracellular Ca^{2+} release, rather then Ca^{2+}-induced Ca^{2+} release via ryanodine

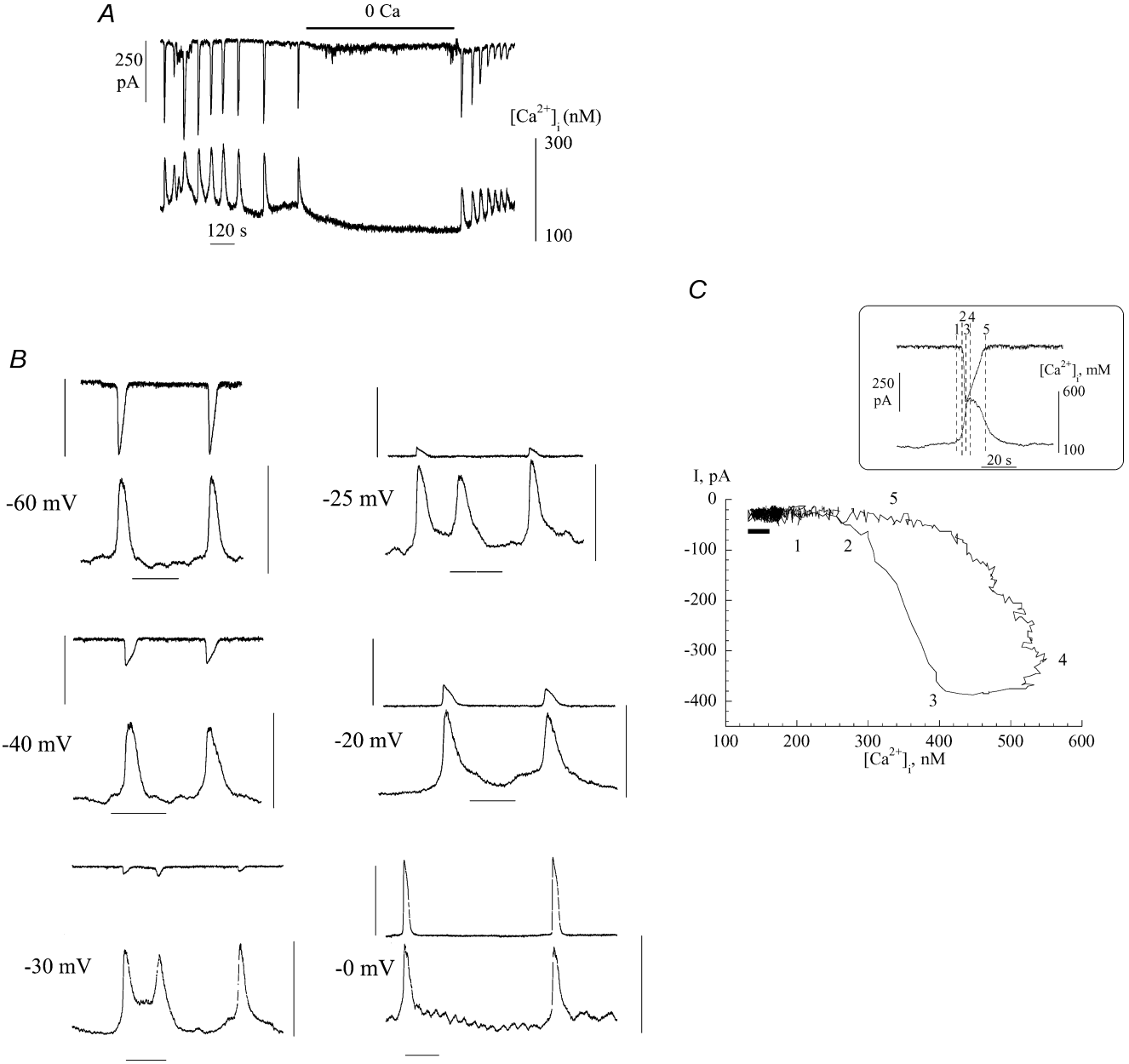

Figure 3. Spontaneous currents and Ca^{2+}-transients in suburothelial myofibroblasts
A, simultaneous recording of inward currents and $[Ca^{2+}]_i$; holding potential −60 mV. *B*, voltage dependence of spontaneous currents and Ca^{2+}-transients; the holding potential is denoted beside each pair of traces. Vertical bars: 400 pA for upper trace, 100–600 nM $[Ca^{2+}]_i$ for lower trace; horizontal bar: 1 minute. *C*, phase-plane plot of the relationship between current and $[Ca^{2+}]_i$. The recordings used to generate the plot are shown in the box, the numbers refer to different times within the plots. The horizontal black bar below the left limb of the plot shows the inherent noise in the traces used to generate the plot. The thickness of the line represents the variance of current noise; the length is the variance of the $[Ca^{2+}]$ signal noise. Because the change of $[Ca^{2+}]$, before current is evoked, is greater than the length of this bar the observation that $[Ca^{2+}]$ changes before current is generated is a real phenomenon and not a random event due to variations of noise in the signals.

receptors from intracellular stores. Figure 6 shows an experiment in which low molecular weight heparin (4 mg ml^{-1}) was included in the patch pipette, and after attainment of membrane rupture would diffuse into the sarcoplasm. Immediately after membrane rupture and a voltage-clamp to −60 mV, exposure to 100 μM ATP generated a Ca^{2+} transient and inward current. Successive exposures to ATP generated decreasing transients until after the third exposure they were completely suppressed. Subsequent exposure to the Ca^{2+} ionophore ionomycin (10 μM) could, however, generate a Ca^{2+} transient and inward current demonstrating that gradual abolition of these phenomena was not due to cell damage. Similar observations were made in three cells. In three different cells superfusion with 100 or 200 μM TMB-8 HCl similarly suppressed Ca^{2+} transients evoked by 100 μM ATP.

The dependence of membrane current on changes to $[Ca^{2+}]_i$ was further tested by raising $[Ca^{2+}]_i$ by other mechanisms than addition of ATP. Thapsigargin will raise $[Ca^{2+}]_i$ by preventing uptake into intracellular stores. Figure 6*B* shows that in a cell clamped at −60 mV ionomycin (10 μM) and then thapsigargin (1 μM) both increased $[Ca^{2+}]_i$, and evoked an inward current after a delay. The rise of intracellular $[Ca^{2+}]$ with thapsigargin was very rapid and suggests that intracellular stores have a rapid exchange of Ca^{2+} with the sarcoplasm.

Purinergic receptor modulators and cholinergic agonists

Figure 7*A* shows that the P2X agonist α,β-methylene ATP (ABMA) was unable to mimic the effect of ATP in generating an intracellular Ca^{2+} transient. Exposure to 100 μM ABMA generated neither a Ca^{2+} transient nor ionic current, whereas 100 μM ATP applied immediately afterwards was able to elicit responses. A pair of spontaneous transients was also observed after the ATP-induced events. Similar results were seen in 17 cells, although in one cell, ABMA did elicit similar responses to ATP. This is in contrast to detrusor smooth muscle where both agonists elicit equivalent Ca^{2+} transients. The lack of action of ABMA, along with the lack of membrane potential changes that precede the Ca^{2+} transient, suggest that the purinoceptors are not ionotropic and may be of the P2Y family.

Figure 7*B* shows however, that 30 μM UTP was able to evoke a Ca^{2+} transient and accompanying inward current, equally effectively as 100 μM ATP; similar results were seen in 25 cells. Suramin (1 mM) partially blocked the ATP transient, but PPADS (up to 80 μM) was ineffective in three cells. Thirty micromolar ADP also generated Ca^{2+} transients and inward currents in 11 cells (Fig. 7*C*); these were of similar magnitude to ATP in five cells and of smaller magnitude in the remainder. In three cells 30 μM CTP did not elicit a Ca^{2+} transient. Figure 7*D* shows that the $P2Y_1$ receptor antagonist MRS2179 (30 μM; Boyer *et al.* 1998) had no effect on the ATP-induced Ca^{2+} transient and current, an effect repeated in seven cells.

The acetylcholine analogue carbachol (100 μM) was ineffective in eliciting Ca^{2+} transients or membrane currents. In 15 of 17 cells no events were recorded with this high concentration of the agonist, whilst in two cells small transients were measured. Figure 7*E* show that 100 μM carbachol also did not alter the magnitude of ATP-evoked Ca^{2+} transients. This suggests that cholinergic receptors are absent in these cells.

Ionic nature of the spontaneous and ATP-generated transient currents

The spontaneous and ATP-evoked currents exhibited a reversal potential at values of -25.4 ± 8.5 and -28.7 ± 7.9 mV, respectively. These values were not significantly different and were similar to the equilibrium potential for Cl^- under these experimental conditions. To strengthen the hypothesis that the transient currents were carried by Cl^-, experiments were repeated in a low extracellular-Cl^- solution (10.6 mM). Figure 8*A* shows ATP-evoked currents in the low-Cl^- solutions; now the reversal potential is at positive potentials, in contrast to the situation in normal-Cl^- solution (e.g. Figure 2*C*). Similar findings were observed for spontaneous currents in the low-Cl^- solution. Figure 8*B* shows summary current-voltage relationships for spontaneous and ATP-evoked currents in normal and low-Cl^- solutions. In the low-Cl^- solution E_{rev} values were $+18.3 \pm 3.7$ mV ($n = 6$) and $+18.1 \pm 4.0$ mV ($n = 6$) and the slope conductances, g, were 0.51 ± 0.19 and 0.80 ± 0.26 nS pF^{-1}, respectively. The E_{rev} and g values were not different for the spontaneous and ATP-induced

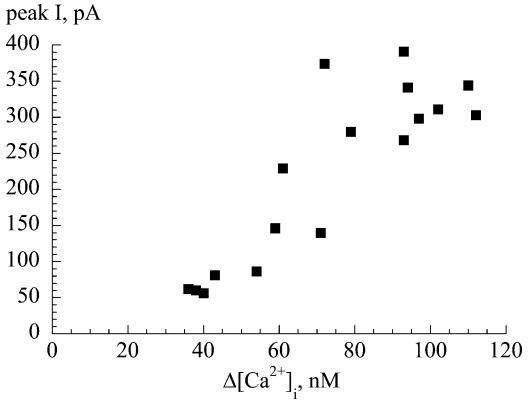

Figure 4. Relationship between the peak inward current and change of the intracellular $[Ca^{2+}]$
The plot relates the magnitudes of the two phenomena during a series of spontaneous transients recorded from a suburothelial myofibroblast. Cell held under voltage-clamp at −60 mV with a K^+-filled pipette.

responses in low-Cl^- solution. However, the E_{rev} values for both spontaneous and ATP-evoked currents were significantly more positive in the low Cl^- solution – the mean values by 43.7 and 45.8 mV, respectively.

Figure 9 shows the effect of the Cl^- channel blocker 1.2 mM DIDS on the current elicited during spontaneous transients. Figure 9*A* shows that DIDS reversibly attenuated spontaneous transients, in this case when the membrane potential was held at 0 mV, although equivalent results were seen regardless of the membrane potential. Similar results were obtained with 0.5 mM SITS and 100 μM niflumic acid ($n = 3$). Niflumic acid at 1 μM had no effect and 10 μM partially attenuated the currents. Figure 9*B* shows the effect of DIDS on current elicited during voltage ramps (0.16 V s^{-1}) between −80 and 60 mV imposed during quiescent periods. The total current was reversibly attenuated by DIDS. Over this more extended range of clamp potentials the outwardly rectifying nature of the current was seen more clearly. The line through the current trace in control solution (Fig. 9*B*) was fitted using Eyring's rate theory (see Methods) for a single barrier pore (Eyring, 1936). The value of the parameter γ in this example was 0.96, and places the barrier on the inner face of the membrane. A similar value of the parameter was seen in five cells. In five separate experiments niflumic acid did not affect spontaneous Ca^{2+} transients, or those evoked by ATP, in the same way as it altered the ionic currents. This lends further support to the argument that the generation of Ca^{2+} transients is not dependent on the presence of these ionic currents.

Discussion

The cells used in these experiments have many characteristics of myofibroblasts (Powell *et al.* 1999); they stained for vimentin and previous work has shown electron

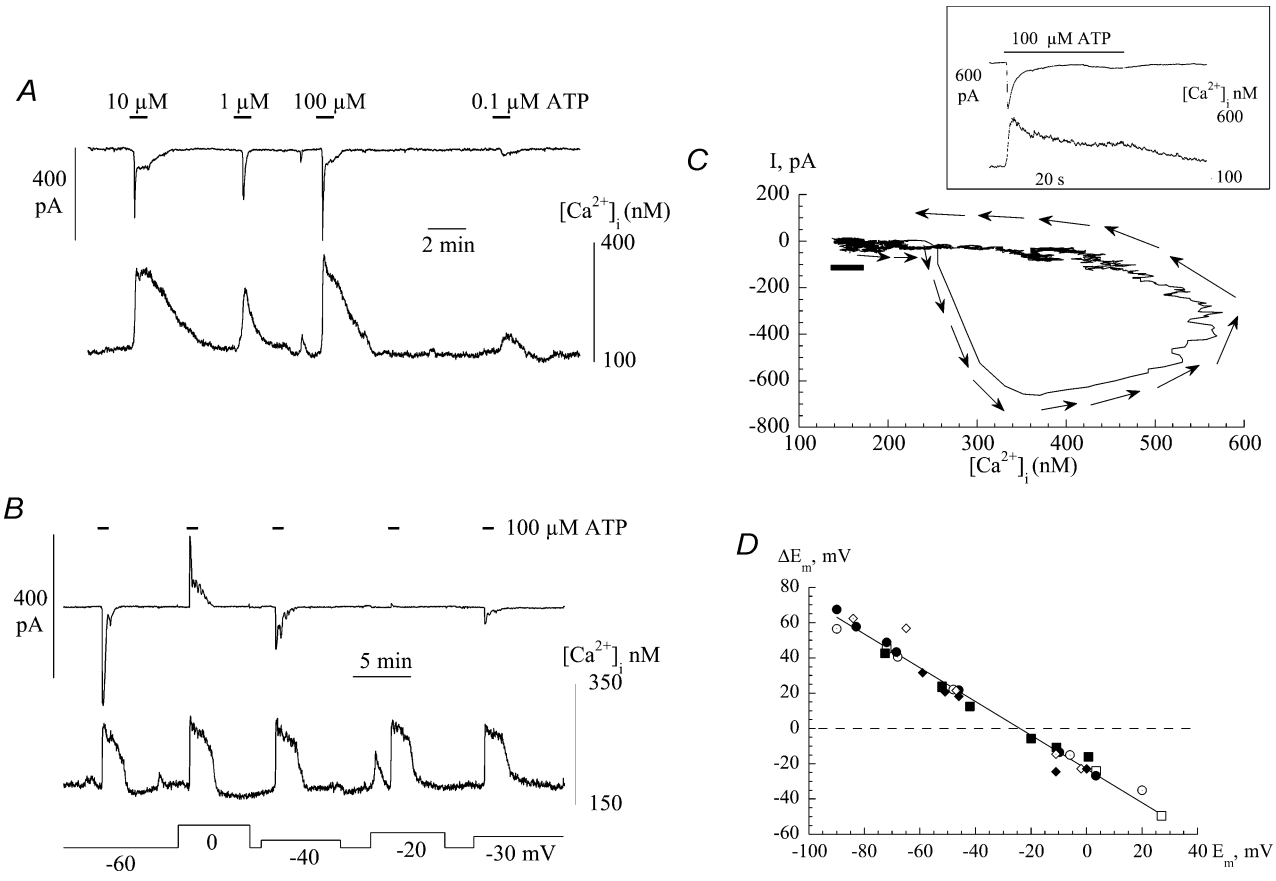

Figure 5. ATP-induced Ca^{2+} transients and spontaneous currents in suburothelial myofibroblasts
A, the effect of ATP in concentrations ranging from 0.1 to 100 μM ATP was added during the periods indicated by the horizontal bars. Cell voltage-clamped at −60 mV with a Cs^+-filled pipette. *B*, voltage dependence of Ca^{2+} transients and spontaneous currents induced by 100 μM ATP. Membrane potential was varied between −60 and 0 mV. *C*, phase-plane plot of the relationship between current and intracellular $[Ca^{2+}]$. The recordings used to generate the plot are shown in the box; arrows indicate the direction of time. The horizontal black bar below the left limb of the plot shows the inherent noise in the traces used to generate the plot. *D*, the relationship between the change of membrane potential, ΔE_m, and the initial value, E_m, upon addition of 100 μM ATP. The straight line was calculated by least squares analysis Data are from six separate cells are shown as indicated by different symbols.

microscopical features such as an incomplete basal lamina and the presence of gap junctions composed of connexin43 (Sui *et al.* 2002). We prefer not to call them interstitial cells, although they have many similar properties, to distinguish them from their obviously different counterparts in the muscular layers of visceral organs, as we do not suggest they have a pacemaking role. Furthermore, these cells do not label for *c-kit*, unlike interstitial cells in the detrusor layer of the guinea-pig bladder (McCloskey & Gurney, 2002). The cells were small compared to detrusor myocytes, as judged by cell capacitance values (Sui *et al.* 2001), so it is unlikely that they are detrusor contaminants from deeper bladder layers.

Electrophysiological characteristics

The membrane characteristics of the myofibroblasts were similar to those previously described (Sui *et al.* 2004) with a large membrane resistance similar to that of detrusor myocytes (Sui *et al.* 2001). Although the distribution of values showed a significant tail of larger numbers, there was no relationship between the presence or the magnitude of any phenomenon described in the Results and the value of membrane resistance or cell size (capacitance). With respect to their functional characteristics suburothelial myofibroblasts form a relatively homogeneous cell group.

The cells were electrically active, generating spike-like depolarizations that did not overshoot but tended to about −25 mV, close to the Cl^- equilibrium potential under these conditions. With K^+-filled patch pipettes, or just after membrane break-through with Cs^+-filled pipettes, the resting potential was about −60 mV; however, after some seconds with the latter pipettes the membrane depolarized to about −30 mV. Two significant conductances in these cells are via Ca^{2+}-activated Cl^- channels and TEA-sensitive (presumably K^+) channels; thus the resting potential lies between the equilibrium potentials of K^+ and Cl^-, whilst the spikes probably represent transient enhancement of Cl^- conductance. Ca^{2+}-activated Cl^- currents have also been described in interstitial cells from the urethral muscular layer (Sergeant *et al.* 2000; Hollywood *et al.* 2003) where they have been postulated to play a pacemaking role.

Modulation of intracellular Ca^{2+}

Spontaneous and agonist-induced Ca^{2+} transients were observed in these cells and this is a consistent observation with those made in interstitial cells from the detrusor layer of the bladder wall and muscle layers of the G-I tract (Ward *et al.* 2000; McCloskey & Gurney, 2002). The Ca^{2+} transients were not a consequence of membrane electrical activity, but rather initiated ionic current through Cl^- channels. This was demonstrated in two ways: the magnitude of the Ca^{2+} transient was independent of ionic current magnitude or polarity; and the rise of intracellular Ca^{2+} always preceded the onset of ionic current. The Ca^{2+} transients were dependent on extracellular Ca^{2+}, as evidenced by their abolition in nominally Ca^{2+}-free solution and their initiation by the Ca^{2+} ionophore ionomycin. However, it is unlikely that transmembrane Ca^{2+} flux generated the Ca^{2+} transient, unless this occurred by an electro-neutral process. Rather it is more likely that intracellular stores were the source of Ca^{2+}, as indicated by the ability of thapsigargin to raise intracellular Ca^{2+}. A similar scheme has been proposed in G-I tract interstitial cells that involved intracellular Ca^{2+} regulation via endoplasmic reticulum IP_3 receptors and mitochondria (Ward *et al.* 2000).

A key observation was that ATP evoked similar Ca^{2+} transients and ionic currents to their spontaneous counterparts. However, ATP did not act through ionotropic P2X receptors, as the responses were not replicated by ABMA, and furthermore Ca^{2+} transients were independent of membrane potential. This is in contrast to detrusor smooth muscle where ABMA can generate Ca^{2+} transients, preceded by membrane depolarization (Wu *et al.* 1999). The ability of UTP and ADP also to generate Ca^{2+} transients suggests the involvement of metabotropic P2Y receptors (Ralevic &

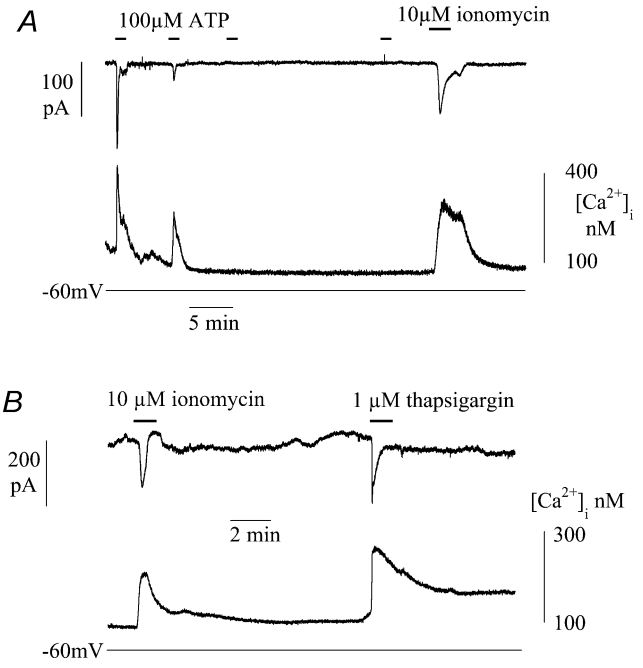

Figure 6. Intracellular pathways for Ca^{2+} release and uptake in suburothelial myofibroblasts

A, Ca^{2+} transients and inward currents during infusion of intracellular low molecular mass heparin by four successive exposures to 100 μM ATP (indicated by horizontal bars). After the last ATP exposure the cell was superfsed with 10 μM ionomycin and the effect of 10 μM ionomycin. *B*, the effects of 10 μM ionomycin and 1 μM thapsigargin. Cells voltage-clamped with Cs^+-filled pipettes at −60 mV.

Burnstock, 1998). The inability of MRS2179 to block the responses would argue against a $P2Y_1$ receptor and the responses to UTP would suggest a $P2Y_2$ or $P2Y_4$ subtype. The profile of actions of CTP, suramin and PPADS is consistent more with a $P2Y_2$ phenotype (Kennedy *et al.* 2000; Wildman *et al.* 2003; King & Townsend-Nicholson, 2004). However, the effectiveness of ADP is not entirely consistent with the above profile, as many studies (but not all, e.g. Bogdanov *et al.* 1998) have shown that ADP is not an agonist for $P2Y_2$ and $P2Y_4$ receptors, and in addition the potency of various agonists differs between species (e.g. Kennedy *et al.* 2000). One possibility is that the receptors are heteromers so that a unique profile is difficult to construct pharmacologically. Therefore, we feel that an unequivocal conclusion about the P2Y receptor subtype is difficult from such observations alone, but should be used to guide further characterization by immunohistochemical methods. However, the important conclusion is that these purinoceptors are different from those on the underlying detrusor or afferent fibres.

These myofibroblasts also showed no responses to cholinergic agonists, again in contrast to bladder interstitial cells (McCloskey & Gurney, 2002). Non-neuronal, epithelial acetylcholine has been proposed in urinary tract tissues as a signalling molecule (Wessler *et al.* 1998). However, it is unknown if this system

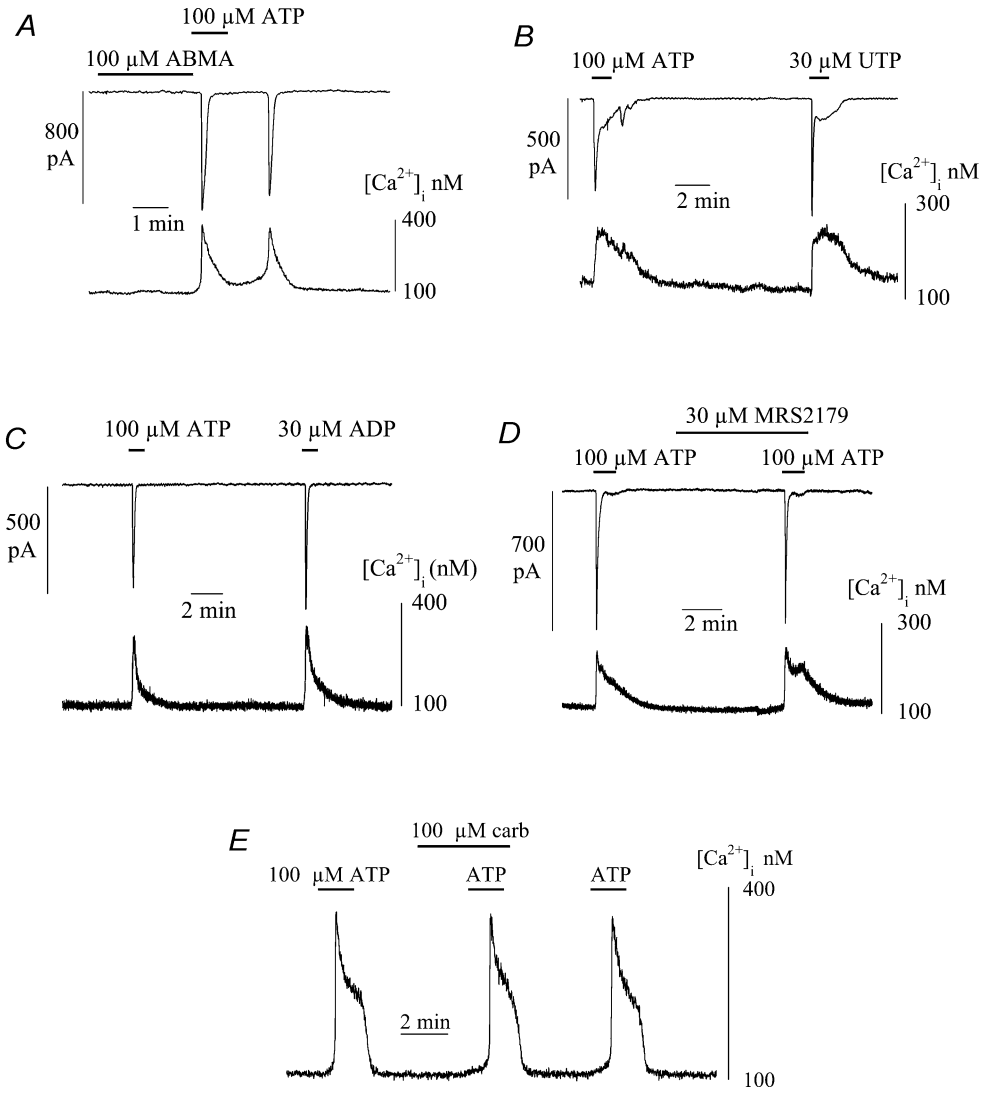

Figure 7. The actions of purinergic receptor agonists and antagonists and carbachol on intracellular $[Ca^{2+}]$ and membrane currents in suburothelial myofibroblasts
A, effects of α,β-methylene-ATP (ABMA) and ATP (100 μM). *B*, actions of 100 μM ATP and 30 μM UTP. *C*, actions of 100 μM ATP and 30 μM ADP. *D*, ATP Ca^{2+} transients in the presence of the $P2Y_1$ receptor antagonist MRS2179 (30 μM). *E*, ATP-induced Ca^{2+}-transients in the presence of carbachol (100 μM). All agents added where indicated by the horizontal bars; cells voltage-clamped at −60 mV with Cs^+-filled pipettes.

has a role in bladder sensation due to the absence of muscarinic responses on these myofibroblasts, and a lack of information about their distribution on bladder afferents.

In addition the duration of the ATP-induced Ca^{2+} transients was generally longer than the current trace, although this was not true when spontaneous events were compared. One possibility is that spontaneous Ca^{2+} release may be more from submembrane locations when there is a much closer relationship between the two variables, whereas ATP-induced release is from deeper Ca^{2+}-store sites, so that changes of bulk $[Ca^{2+}]$ are more dissociated from subsarcolemmal changes. This hypothesis is currently being investigated.

Physiological significance of the suburothelial myofibroblast layer

The simplest hypothesis of bladder sensation is that ATP, released from the urothelium when subjected to changes of hydrostatic pressure, activates urothelial and suburothelial afferents via $P2X_3$ receptors (Ferguson *et al.* 1997; Cockayne *et al.* 2000). The identification of a suburothelial layer of myofibroblasts that also responds to ATP through P2Y receptors suggests that this intermediate layer of cells may exert a modulatory effect on this process. There have been to our knowledge no studies concerning the localization of P2Y receptors on urinary bladder epithelium. These cells are the main site of the gap junction protein connexin43 in the bladder wall (Sui *et al.* 2002). This and the demonstration of gap junctions between adjacent cells suggest that this cell layer forms a functional syncytium located between the urothelium and bladder afferents. Previous cable calculations have estimated that focal depolarization of this cellular network can depolarize a surrounding area of several hundred micrometres (Sui *et al.* 2004).

Two possible roles for the ATP-mediated responses in suburothelial myofibroblasts are that they modulate the effect of ATP on activation of the primary afferent fibres, and/or they influence urothelial cells themselves as a feedback control. With respect to the first role, exogenous ATP would elicit a rise of intracellular Ca^{2+}, and/or modulate pre-existing spontaneous activity. This would contract the myofibroblast, as well as influence the behaviour of neighbouring cells. Because myofibroblasts make such intimate contact with afferent endings (Wiseman *et al.* 2003), their contraction would be expected to modulate afferent activity. Stretch activation of afferents has been observed in the gut wall, for example (Furness *et al.* 1998). This model suggests that myofibroblasts modulate afferent activity and this introduces a variable gain stage in the sensory process. Such a model has a number of advantages:

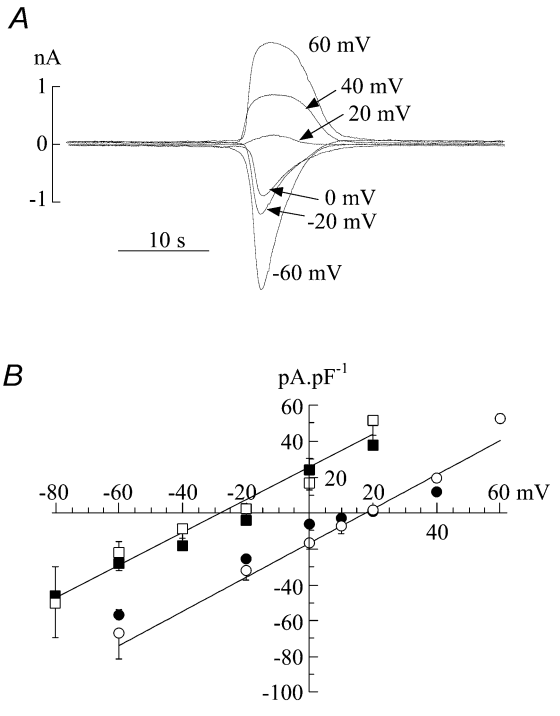

Figure 8. Cl^- dependence of spontaneous and ATP-induced spontaneous currents
A, superimposed current transients from the same cell, elicited by 100 μM ATP at different holding potentials in low-extracellular Cl^- solution (10.6 mM). Current–voltage relationships of ATP-induced (filled symbols) and spontaneous (open symbols) currents in normal extracellular $[Cl^-]$ (squares) and low extracellular $[Cl^-]$ (circles). All experiments used Cs^+-filed pipettes.

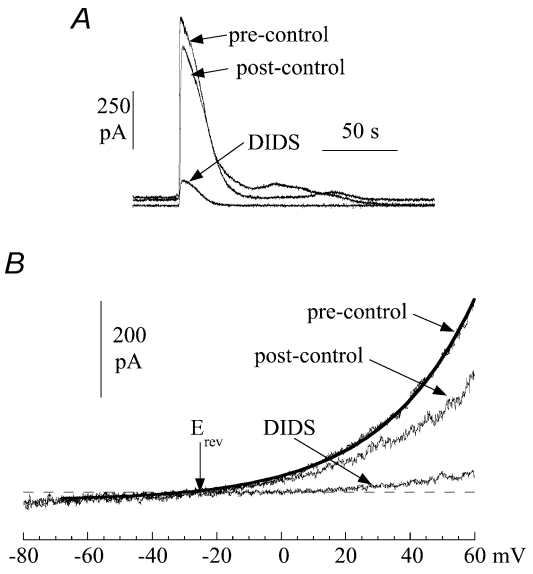

Figure 9. The action of DIDS (1.2 mM) on spontaneous currents in suburothelial myofibroblasts
A, three superimposed transients from a continuous recording. *B*, current–voltage relationship of membrane current during a quiescent phase. Membrane potential was changed as a ramp (0.16 V s^{-1}). The line through the pre-control data was best-fitted using eqn (1) (Methods) and the reversal potential, E_{rev}, indicated. Cells were voltage-clamped at 0 mV with a Cs^+-filled pipette.

modulation of myofibroblast activity itself will increase the gain of the system, and this may provide one role for the nitrergic fibres that innervate these types of cell (Smet *et al.* 1996); the syncytial nature of the network will provide peripheral filtering of the signal; and alteration of myofibroblast activity by other factors may explain different levels of sensation under different conditions.

The role of P2Y receptors in somatosensation has been reported elsewhere where it has been shown that such receptors mediate the response of vanilloid-receptor activation by ATP in dorsal rot ganglion cells, or expression systems (Tominaga *et al.* 2001; Moriyama *et al.* 2003). These authors also speculated that a P2Y mechanism would modulate a sensory system based on an ionotropic P2X-receptor activation.

It remains to be ascertained what the functions are of the secondary depolarizations that accompany the transient increase of the intracellular $[Ca^{2+}]$, either in the primary cell or in neighbouring cells of the functional syncytium. The failure to elicit consistently transient Ca^{2+} currents in these myofibroblasts does not suggest that depolarization elicits Ca^{2+} influx by these routes. However, the dependence of the Ca^{2+} transients on extracellular Ca^{2+} does suggest some mode of transmembrane Ca^{2+} flux and it remains a primary objective to determine how the membrane potential regulates Ca^{2+} homeostasis in these cells.

References

Bogdanov YD, Wildman SS, Clements MP, King BF & Burnstock G (1998). Molecular cloning and characterisation of rat P2Y4 nucleotide receptor. *Br J Pharmacol* **124**, 428–430.

Boyer JL, Mohanram A, Camaioni E, Jacobson KA & Harden TK (1998). Competitive and selective antagonism of P2Y1 receptors by N6-methyl 2′-deoxyadenosine 3′,5′-bisphosphate. *Br J Pharmacol* **124**, 1–3.

Cockayne DA, Hamilton SG, Zhu Q-M, Dunn PM, Zhong Y, Novakovic S, Malmberg AB, Cain G, Berson A, Kassotakis L, Hedley L, Lachnit WG, Burnstock G, McMahon SB & Ford APD (2000). Urinary bladder hyporeflexia and reduced pain-related behaviour in P2X3-deficient mice. *Nature* **407**, 1011–1015.

De Groat WC & Yoshimura N (2001). Pharmacology of the lower urinary tract. *Ann Rev Pharmacol Toxicol* **41**, 691–721.

Donovan J, Naughton M, Gotoh M, Corcos J, Jackson S, Kelleher C, Lukacs B & Costa P (1999). Symptom and quality of life assessment. In *Incontinence*, ed. Abrams P, Khoury S & Wein A, pp. 295–331. Health Publications Ltd, Plymouth, UK.

Eyring H (1936). Viscosity, plasticity and diffusion as examples of absolute reaction rates. *J Chem Phys* **4**, 283–291.

Ferguson DR, Kennedy I & Burton TJ (1997). ATP is released from rabbit urinary bladder epithelial cells by hydrostatic pressure changes-a possible sensory mechanism. *J Physiol* **505**, 503–511.

Fowler CJ (2002). Bladder afferents and their role in the overactive bladder. *Urology* **59** (5 Suppl. 1), 37–42.

Fry CH & Langley SE (2001). *Ion-Selective Electrodes in Biological Systems*. Harwood Press, London.

Furness JB, Kunze WA, Bertrand PP, Clerc N & Bornstein JC (1998). Intrinsic primary afferent neurons of the intestine. *Prog Neurobiol* **54**, 1–18.

Hollywood MA, Sergeant GP, McHale NG & Thornbury KD (2003). Activation of Ca^{2+}-activated Cl^- current by depolarizing steps in rabbit urethral interstitial cells. *Am J Physiol* **285**, C327–C333.

Kennedy C, Qi AD, Herold CL, Harden TK & Nicholas RA (2000). ATP, an agonist at the rat $P2Y_4$ receptor, is an antagonist at the human $P2Y_4$ receptor. *Mol Pharmacol* **57**, 926–931.

King BF & Townsend-Nicholson A (2004). Nucleotide and nucleoside receptors. Life Science Reviews at http://www.tocris.com (Technical Support and Resources).

Kumar V, Chapple CR & Chess-Williams R (2004). ATP release from urothelium of bladders with sensory disorders. *BJU Int* (in Press).

Lee HY, Bardini M & Burnstock G (2000). Distribution of P2X receptors in the urinary bladder and the ureter of the rat. *J Urol* **162**, 2002–2007.

McCloskey KD & Gurney AM (2002). Kit positive cells in the guinea pig bladder. *J Urol* **168**, 832–836.

Montgomery BSI & Fry CH (1992). The action potential and net membrane currents in isolated human detrusor smooth muscle cells. *J Urol* **147**, 176–184.

Moriyama T, Iida T, Kobayashi K, Higashi T, Fukuoka T, Tsumura H, Leon C, Suzuki N, Inoue K, Gachet C, Noguchi K & Tominaga M (2003). Possible involvement of $P2Y_2$ metabotropic receptors in ATP-induced transient receptor potential vanilloid receptor 1-mediated thermal hypersensitivity. *J Neurosci* **23**, 6058–6062.

Powell DW, Mifflin RC, Valentich JD, Crowe SE, Saada JI & West AB (1999). Myofibroblasts. I. Paracrine cells important in health and disease. *Am J Physiol* **277**, C1–C19.

Ralevic V & Burnstock G (1998). Receptors for purines and pyrimidines. *Pharmac Rev* **50**, 415–492.

Sergeant GP, Hollywood MA, McCloskey KD, Thornbury KD & McHale NG (2000). Specialised pacemaking cells in the rabbit urethra. *J Physiol* **526**, 359–366.

Smet PJ, Jonavicius J, Marshall VR & de Vente J (1996). Distribution of nitric oxide synthase-immunoreactive nerves and identification of the cellular targets of nitric oxide in guinea-pig and human urinary bladder by cGMP immunohistochemistry. *Neuroscience* **71**, 337–348.

Sui GP, Rothery S, Dupont E, Fry CH & Severs NJ (2002). Gap junctions and connexin expression in human sub-urothelial interstitial cells. *BJU Int* **90**, 118–129.

Sui GP, Wu C & Fry CH (2001). The electrophysiological properties of cultured and freshly isolated detrusor smooth muscle cells. *J Urol* **165**, 621–626.

Sui GP, Wu C & Fry CH (2004). Electrical characteristics of sub-urothelial cells isolated from the human bladder. *J Urol* **171**, 938–943.

Tominaga M, Wada M & Masu M (2001). Potentiation of capsaicin receptor activity by metabotropic ATP receptors as a possible mechanism for ATP-evoked pain and hyperalgesia. *Proc Natl Acad Sci U S A* **98**, 6951–6956.

Ward SM, Ördög T, Koh SD, Abu Baker S, Jun JY, Amberg G, Monaghan K & Sanders KM (2000). Pacemaking in interstitial cells of Cajal depends upon calcium handling by endoplasmic reticulum and mitochondria. *J Physiol* **525**, 355–361.

Weidmann S (1970). Electrical constants of trabecular muscle from mammalian heart. *J Physiol* **210**, 1041–1054.

Wessler I, Kirkpatrick CJ & Racké K (1998). Non-neuronal acetylcholine, a locally acting molecule, widely distributed in biological systems: Expression and function in humans. *Pharmacol Therap* **77**, 59–79.

Wildman SS, Unwin RJ & King BF (2003). Extended pharmacological profiles of rat $P2Y_2$ and rat $P2Y_4$ receptors and their sensitivity to extracellular H^+ and Zn^{2+} ions. *Br J Pharmacol* **140**, 1177–1186.

Wiseman OJ, Fowler CJ & Landon DN (2003). The role of the human bladder lamina propria myofibroblast. *BJU Int* **91**, 89–93.

Wu C, Bayliss M, Newgreen D, Mundy AR & Fry CH (1999). A comparison of the mode of action of ATP and carbachol on isolated human detrusor smooth muscle. *J Urol* **162**, 1840–1847.

Wu C & Fry CH (2001). Evidence for Na^+/Ca^{2+} exchange and its role in intracellular Ca^{2+} regulation in guinea-pig detrusor smooth muscle cells. *Am J Physiol* **280**, C1090–C1096.

Wu C, Sui GP & Fry CH (2002). The role of the L-type Ca^{2+} channel in refilling functional intracellular Ca^{2+} stores in guinea-pig detrusor smooth muscle. *J Physiol* **538**, 357–369.

Acknowledgements

We wish to thank The Wellcome Trust and St Peter's Trust for financial assistance.